EFFECT OF WAVE-LIKE BODY FORCE CONTROL ON REATTACHMENT LENGTH IN BACKWARD-FACING STEP TURBULENT FLOW

Junichi Morita, Hiroya Mamori, Takeshi Miyazaki
Department of Mechanical and Intelligent Systems Engineering
The University of Electro-Communications
1-5-1, Chofugaoka, Chofu, Tokyo 182-8585, Japan
mamori@uec.ac.jp

ABSTRACT

Direct numerical simulations of incompressible turbulent flows over a backward-facing step are performed. To control the flow separation, a spanwise uniform traveling wave-like body force control and a wave-machine-like traveling body force control are given on the top of the step. The effect of wavespeed in both controls is investigated. The wavespeed is one of the control parameters. In the controlled flow, a time-averaged reattachment length is affected by the control, e.g., when the wave travels in the downstream direction, the time-averaged reattachment point moves in the upstream direction.

INTRODUCTION

The flow separation and reattachment can be frequently found in our living environment (e.g., the flows around vehicles and buildings, etc.). However, an energy loss occurs at the flow separation point due to the increased velocity and pressure fluctuations caused by the vibration of the separation bubble. On the one hand, since the turbulence is promoted, these phenomena help to improves heat transfer and enhances mixing effects. Therefore, understanding both phenomena is required in engineering design.

The flow over the backward-facing step (BFS), in which there is only one separation region with reattachment, has been studied well due to its simplicity. In particular, the reattachment length has been investigated extensively because of the occurrence of important engineering phenomena (i.e., the increased pressure resistance, the accelerated heat transfer, the noise generation, etc.). Ötügen (1991) investigated the effect of the expansion ratio ER on the reattachment length, and this experiment showed that the reattachment length increases with increasing ER. Recently, Nadge & Govardhan (2014) conducted a parametric study to comprehensively investigate the effects of the expansion ratio and Reynolds number on the reattachment length.

Several methods for controlling the turbulent flow have been proposed, and one of them, traveling wave control, has a high drag reduction effect. Min *et al.* (2006) performed a direct numerical simulation to investigate the effect of traveling wave blowing and suction control in a channel flow. They achieved a drag reduction rate of about 30% by upstream traveling waves. It is known that the upstream traveling wave in blowing and suction has the pumping effect (Hœpffner & Fukagata (2009)). However, since blowing and suction are difficult to make practical, Mamori & Fukagata (2014) generated traveling waves by body force and investigated the effect of this control in a turbulent channel flow. They reported that the pumping effect of the traveling wave enhanced the vortical structures.

It is known that the separation bubbles have a great influence on the oscillation of the reattachment length (Schäfer *et al.*, 2009). Therefore, we expect that the pumping effect of the traveling wave control will enhance the mixing of the separation bubbles, which will reduce the reattachment length. Morita *et al.* (2022) reported that a traveling wave-like body force control reduces the reattachment length in the BFS turbulent flow. The traveling wave control had a uniform input in the spanwise direction. In order to reduce the reattachment length further, it is necessary to promote turbulence in the recirculation region, and we employ a wave-machine-like traveling wave (Nabae & Fukagata, 2020). The control has spatial periodicity in the spanwise direction, which is expected to promote turbulence and affect the reattachment length.

In this study, we perform direct numerical simulations of the turbulent flows over the backward-facing step. To control the flow separation, the spanwise uniform traveling wave-like body force and the wave-machine-like traveling body force are applied to the top of the step. The purpose of this study is to investigate the effect of the controls on the reattachment length and to clarify the mechanism. Especially, the effect of the wavespeed is discussed in this paper.

Direct Numerical Simulation

Direct numerical simulations of turbulent flows over the backward-facing step are performed. The governing equations are incompressible continuity and Navier-Stokes equations, and these equations are defined as follows,

$$\frac{\partial u_i}{\partial x_i} = 0, \tag{1}$$

$$\frac{\partial u_i}{\partial t} + u_j \frac{\partial u_i}{\partial x_j} = -\frac{\partial p}{\partial x_i} + \frac{1}{\mathrm{Re_b}} \frac{\partial^2 u_i}{\partial x_j^2} + f_i, \tag{2}$$

where, x_i u_i, and f_i ($i = 1 \sim 3$) are the coordinates, the velocities, and the body force term in the streamwise, wall-normal and spanwise direction, respectively. In addition, t is time, and p is pressure. The coordinates are interchangeably used as x, y and z, the corresponding velicity components are used as u, v and w, respectively, The Reynolds number defined by the channel half-width at the inlet δ and the inflow bulk velocity $2u_b$ is $\mathrm{Re_b} = 2u_b^*\delta^*/\nu^* = 5600$. Here, the asterisk denotes the

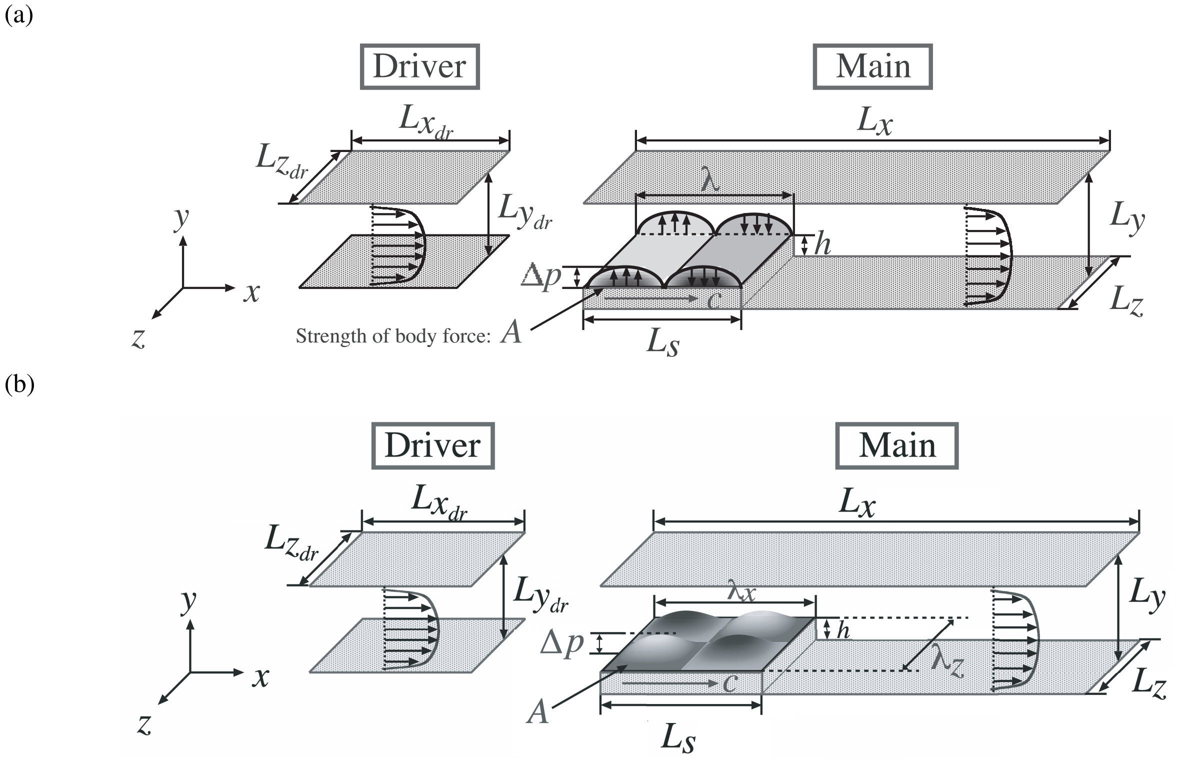

Figure 1. Computaional domain of the flow over the backward-facing step with (a) the spanwise uniform traveling wave-like body force and (b) the wave-machine-like traveling body force.

dimensional variable. The flow condition is the constant flow rate.

We employ the DNS code for the channel flows by Fukagata & Kasagi (2006). The governing equations are discretized using an energy-conserving second-order accurate central difference method for space. For time integration, the second-order accurate Crank- Nicolson scheme and the low-storage third-order accurate Runge–Kutta scheme are used.

Figure 1 shows the computational domain of the backward-facing step flow and the driver. Here, the driver is the fully developed turbulent channel flow and is used to define the inflow velocity of the turbulent flow over the backward-facing step. The computational domain is set to $(L_x, L_y, L_z) = (6\pi, 2.4, \pi)$ and $(L_x^d, L_y^d, L_z^d) = (2\pi, 2, \pi)$, and the number of grids is set to $(N_x, N_y, N_z) = (768, 128, 128)$ and $(N_x^d, N_y^d, N_z^d) = (128, 96, 128)$. The streamwise length in a step is $L_s = 2\pi$, the step height is $h = 0.4$. The expansion ratio is $ER = L_y/(L_y - h) = 1.2$. The superscript d denotes the physical quantity at the driver.

In the boundary condition of the backward-facing step flow, the periodic boundary condition is applied in z-direction. As the inflow velocity, we use the velocity distribution of the fully developed flow generated in the driver part. The convection condition is imposed on the outlet. The non-slip condition is imposed on the wall. The step is represented by the immersed boundary method proposed by Kim *et al.* (2001). They used the fractional-step method, while the authors used the SMAC method. In the driver, we impose periodic boundary conditions in x and z directions and, the no-slip condition on the wall.

In order to control the flow separation, we apply the spanwise uniform traveling wave-like body force and the wave-machine-like traveling body force on the top of the step (Fig. 1). Since the body acts in the region near the wall, the body force control is assumed to exponentially decay along the wall-normal direction. Therefore, each controls are defined as,

$$f_y = A \exp\left(-\frac{y-h}{\Delta p}\right) \cos\left(\frac{2\pi}{\lambda_x}(x-ct)\right), \tag{3}$$

$$f_y = A \exp\left(-\frac{y-h}{\Delta p}\right) \cos\left(\frac{2\pi}{\lambda_x}(x-ct)\right) \cos\left(\frac{2\pi}{\lambda_z}z\right). \tag{4}$$

The control parameters are the amplitude A, the penetration length Δp, and the wavespeed c. The wavelengths in the main and spanwise directions are λ_x and λ_z, respectively. In this study, we use a parameter set of $A = 2$, $\Delta p = 0.1$, and $\lambda_x = 2\pi$, which significantly reduced the reattachment length in Morita *et al.* (2022). The wavelength in the spanwise direction is fixed at $\lambda_z = \pi$. We investigate the effect of wavespeed c on the reattachment length.

The time averaged skin-friction coefficient C_f on the lower wall of the uncontrolled flow is shown in Fig. 2. The definition of the skin-friction coefficient C_f is,

$$C_f = \frac{\tau_w^*}{\frac{1}{2}\rho^*(2u_b^*)^2}. \tag{5}$$

Here, τ_w^* is the lower wall shear stress, and ρ^* is the density. The horizontal axis is normalized by the step height h, and the origin $x/h = 0$ is the separation point. The reattachment length x_r is the distance from the origin to the reattachment point of $C_f = 0$ (except for the secondary recirculation region).

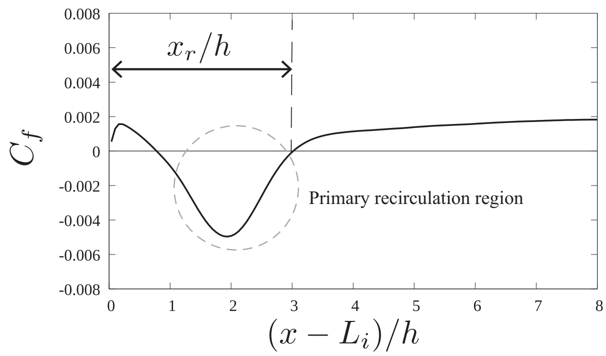

Figure 2. Skin-friction coefficient C_f and reattachment length x_r/h.

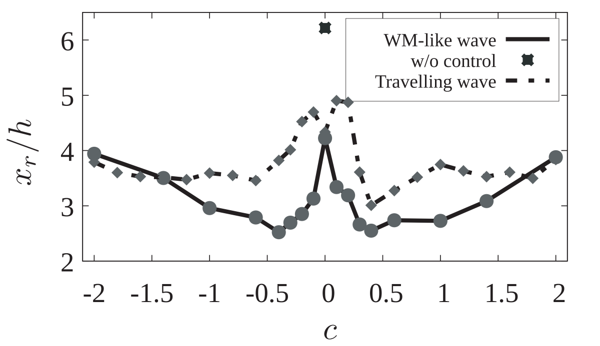

Figure 3. The reattachment length as a function of the wavespeed c.

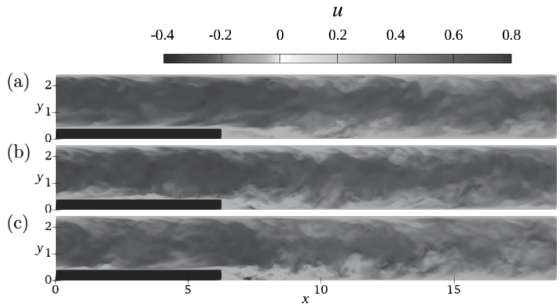

Figure 4. The instantaneous streamwise velocity: (a) w/o control, (b) Case 1, (c) Case 2.

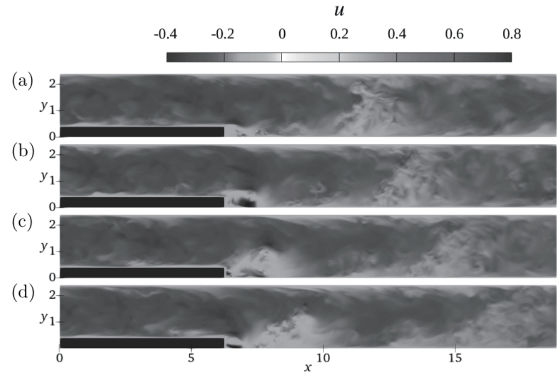

Figure 5. The instantaneous streamwise velocity in Case TW: (a) $t = 500$, (b) $t = 504$, (c) $t = 508$, (d) $t = 512$.

Results and discussion

Figure 3 shows the effect of wavespeed on the reattachment length in the Traveling wave and the WM-like wave. Here, "Traveling wave" means the spanwise uniform traveling wave-like body force, and "WM-like wave" means wave-machine-like traveling body force. Both the Traveling wave and the WM-like wave reduce the reattachment length regardless of the wavespeed. The minimum x_r is obtained at $c = 0.4$ in both contols. The reattachment length of the WM-like wave was shorter than that of the Traveling wave at $-1 < c < 1.5$. In the WM-like wave, the direction of wave propagration had little effect on the reattachment length. On the other hand, the effect of wavespeed in the Traveling wave on the reattachment length was different among the three cases: downstream traveling wave ($c > 0$), upstream traveling wave ($c < 0$), and stationary wave ($c = 0$). For the downstream traveling wave ($c > 0$), the reattachment length is decreased as the wavespeed decrease. For the upstream traveling wave ($c < 0$), the reattachment length is kept constant. Compared with that in the traveling wave ($c \neq 0$), the reattachment length in the stationary wave ($c = 0$) increased.

The effect of the Traveling wave is discussed by comparing the results of the case without the control and the following Case 1 $\sim$ 3: Cases 1, stationary wave-like body force ($c = 0$) as shown in Fig. 1(a); Case 2, stationary wave with the opposite phase to Case 1; Case TW, traveling wave ($c = 0.6$) in the downstream direction.

Figure 4 shows the instantaneous streamwise velocity distribution. In Case 1, the reattachment length and recirculation region decrease because the control generated backward flow on the step and suppressed the velocity near the separation point. In Case 2, the upward flow is induced near the separation point, and the recirculation region is enlarged. This enhanced the fluid mixing caused by the shear between the main flow and the backward flow in the recirculation region. In Case TW, the strong vortical structure is generated in the recirculation region and is released as shown in Fig. 5, which causes a significant decrease in the reattachment length.

Figure 6 shows the distribution of the Reynolds shear stress ($-\overline{u'v'}$). Here, the instantaneous velocity u_i is decomposed into the velocity averaged in the time and spanwise direction $\overline{u_i}$ and the variation u_i'.

$$u_i = \overline{u_i} + u_i' \tag{6}$$

In Case 1, the velocity fluctuation decreases as compared to the uncontrolled case; in Case 2 and Case TW, the velocity fluctuation increases.

In order to investigate the relationship between the release period of the vortical structure and the period of the traveling wave ($T = \lambda/|c|$), we analyze the phase-averaged statistics. The phase average is defined as follows,

$$\langle f \rangle(x,y,\tau) = \frac{1}{N_p}\sum_{n=1}^{N_p}\left[\frac{1}{L_z}\int_0^{L_z} f(x,y,z,\tau+nT)dz\right] \tag{7}$$

where, $\tau = t - nT$ $(0 < \tau < T, n \in \mathbb{Z})$ is the time within one traveling wave cycle. N_p is the number of data used for phase average.

Figure 7 shows the phase-averaged reattachment length in Case TW. It shows the temporal variation of the reattachment length within one cycle of the traveling wave. The separation bubble is released when the reattachment length decreases rapidly. The release period of the separation bubble corresponds with the period of the traveling wave. Therefore, it is considered that the release period of the vortical structure can be controlled by changing the wavelength and wavespeed in the traveling wave-like body force control.

The mechanism of the reattachment length reduction in each case was different. In Case TW, the pumping effect in the traveling wave generated a strong vortical structure in the recirculation region, which caused the release of the vortical structure, thus reducing the reattachment length. Phase analysis showed that the release period of the vortical structure corresponds with the period of the traveling wave. The control effect was different in the stationary wave because the input phase distribution was different. In Case 1, the reverse flow region generated on the step suppressed the velocity near the separation point and the velocity fluctuation in the recirculation region, which caused the reduction of the reattachment length. In Case 2, reattachment length was reduced because of the enhanced mixing of the separation vortical structure, but the recirculation region was enlarged because of the upward flow induced near the separation point. Therefore, the reduction rate of the reattachment length was smaller than those in the other cases.

Figure 8 compares the turbulent vortical structures. The vortical structures are visualized by the isosurface of the second invariant of the velocity deformation tensor (i.e., so-called the Q value). The wavespeed is set at $c = 0.4$ for both cases. In the uncontrolled case, there are many vortical structures in the separation bubble compared with the upper surface of the step. In the Traveling wave, the large and spanwise uniform vortical structure is observed at the top of the step. In the case of WM-like wave, the vortical structures distribute non-uniformly in the spanwise direction, unlike the Traveling wave. In addition, the streamwise vortical structure is generated on the upper surface of the step, which may work as vortex generators. Therefore, the WM-like wave control was more effective in reducing the reattachment length than the spanwise uniform traveling wave because the control generates the streamwise vortical structure on the top surface of the step.

Conclusion

Direct numerical simulations of the incompressible turbulent flow over the backward-facing step are performed. In order to control the separation flow, the spanwise uniform traveling wave-like body force control and wave-machine-like traveling body force are applied to the top surface of the step. In this study, we investigate the effects of wavespeed c on the reattachment length. Compared with the uncontrolled case, the reattachment length decreased in all the control cases. However, the mechanism was different and depended on the control. In the spanwise uniform stationary wave, the control effect was different because the input phase distribution was different. The velocity fluctuation in the recirculation affected the increase or decrease of the reattachment length. In the spanwise uniform cases, the control generated a strong vortical structure in the recirculation region, which caused the release of the vortical structure, thus reducing the reattachment length. The release period of the vortical structure corresponded with the period of the traveling wave. In the WM-like wave control, the control generates the streamwise vortical structure on the top surface of the step. Therefore, mixing of separation bubble is more enhanced and the reattachment distance is shortened.

Acknowledgments

We would like to thank Mr. Kimura for his significant contribution to this research.

REFERENCES

Fukagata, K. & Kasagi, N. 2006 A theoretical prediction of friction drag reduction in turbulent flow by superhydrophobic surfaces. *Physics of Fluid* **18**, 051703.

Hœpffner, J. & Fukagata, K. 2009 Pumping or drag reduction? *Journal of Fluid Mechanics* **635**, 171–187.

Kim, J., Kim, D. & Choi, H. 2001 An immersed-boundary finite-volume method for simulations of flow in complex geometries. *Journal of Computational Physics* **171**, 132–150.

Mamori, H. & Fukagata, K. 2014 Drag reduction effect by a wave-like wall-normal body force in a turbulent channel flow. *Physics of Fluid* **26**, 862–874.

Min, T., Kang, S. M., Speyer, J. L. & Kim, J. 2006 Sustained sub-laminar drag in a fully developed channel flow. *Journal of Fluid Mechanics* **558**, 309–318.

Morita, J., Mamori, H. & Miyazaki, T. 2022 Direct numerical simulation of the backward-facing step turbulent flow controlled by traveling wave-like body force. *International Journal of Heat and Fluid Flow* **95**, 108964.

Nabae, Y. & Fukagata, K. 2020 Parameter dependence of turbulent friction drag reduction effect by wave-machine-like traveling waves. *Nagare (in Japanese)* **39**, 312–315.

Nadge, P. M. & Govardhan, R. N. 2014 High reynolds number flow over a backward-facing step: structure of the mean separation bubble. *Experimental in Fluids* **55**, 1657–1678.

Ötügen, M. V. 1991 Expansion ratio effects on the separated shear layer and reattachment downstream of a backward-facing step. *Exprimental in Fluids* **10**, 273–280.

Schäfer, F., Breuer, M. & Durst, F. 2009 The dynamics of the transitional flow over a backward-facing step. *Journal of Fluid Mechanics* **623**, 85–119.

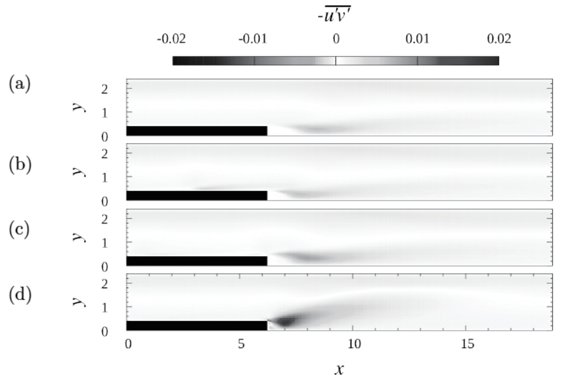

Figure 6. The Reynolds shear stress ($-\overline{u'v'}$): (a) w/o control, (b) Case 1, (c) Case 2, (d) Case TW.

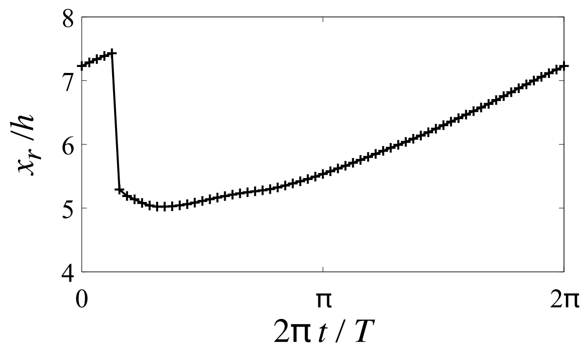

Figure 7. The phase-averaged reattachment length in Case TW.

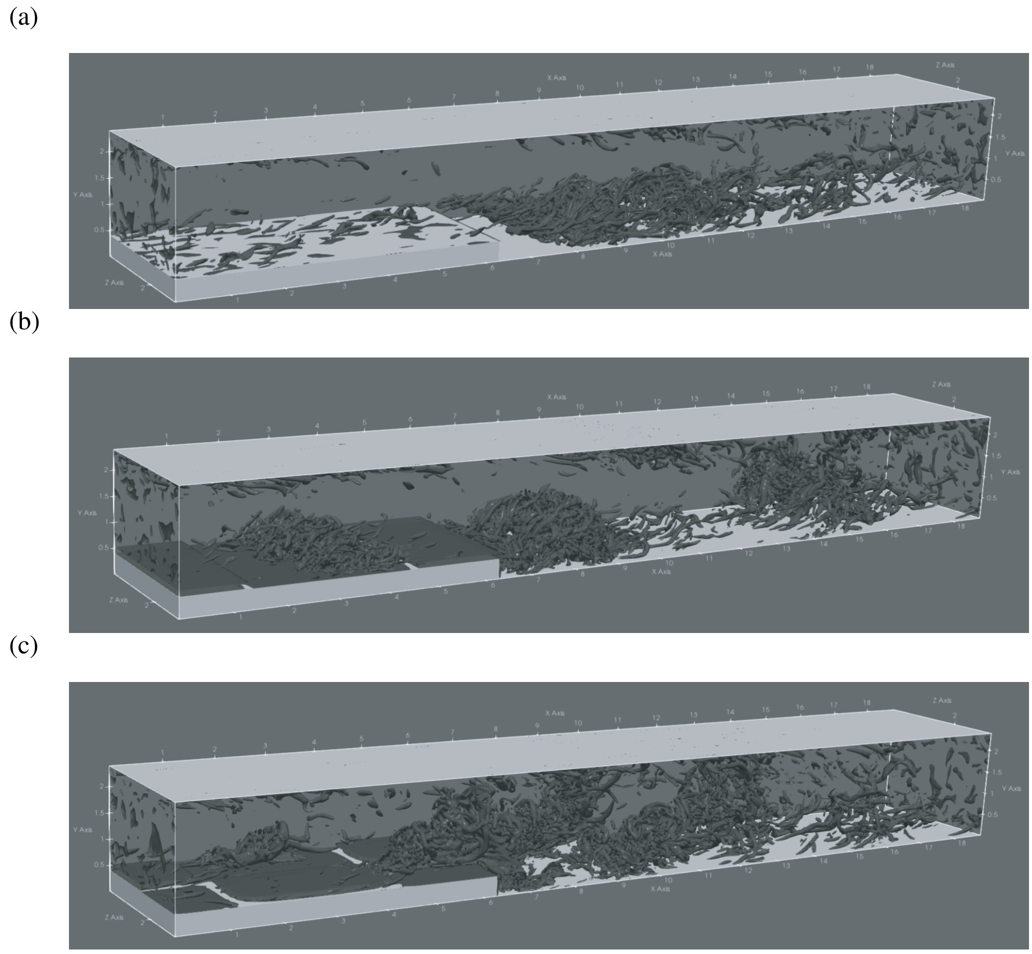

Figure 8. Instantaneous vortical structures of (a) uncontrolled flow, (b) travelling wave at $c = 0.4$, and (c) wave machine-like travelling wave at $c = 0.4$.